Electronic Supplementary Material (ESI) for ChemComm.

1 **Supplementary Data**

2 Oxygen Vacancy Promoted Photocatalytic H_2O_2 Production Over
3 Bismuth Oxybromide Nanosheets

4 Hongxiang Chu,[† a, b, c] Ruofan Li,[† b, c] Di Zeng,[b, c] Wenjing Wang,[c]
5 Bingkun Cui,[b, c] Taikang Jia,[b, c] Ling Zhang,[*b, c] Wenzhong Wang[*a, b, c]

Supplemental Experimental Procedures

Materials

All chemicals were of analytical grade and used as received without further purification.

Catalysts preparation

The BiOBr nanosheets with oxygen vacancies, denoted as BiOBr-Ovs, were prepared through a solvothermal method according to a reference with modification.[22] Typically, 0.97 g bismuth nitrate ($Bi(NO_3)_3 \cdot 5H_2O$) were dissolved in 50 mL mannitol, then 400 mg PVP were added and the system was vigorously stirred for 1 h till fully dissolved. Afterwards, 10 mL saturated KBr aqueous solution was slowly dropped into the above solution under continuous stirring. After stirring for 1 h, the white suspension was transferred to a 100 mL Teflon-lined stainless-steel autoclave and heated at 160 °C for 3 h. After cooling down to room temperature, the obtained precipitates were washed by deionized water and absolute ethanol several times and dried at 60 °C for 12 h. The above solids were grinded to be used.

The BiOBr were prepared by the heat treatment of the BiOBr-Ovs, which were heated up to 500 °C at 4 °C min^{-1} from room temperature and held at 500 °C for 60 min.

Characterization

The X-ray diffraction (XRD) patterns were recorded on a Rigaku Ultima IV X-ray diffractometer with Cu K_α (λ = 0.15418 nm) radiation. The morphology of the samples was observed by a Hitachi SU8220 scanning electron microscopy (SEM). Diffuse reflectance spectra (DRS) were recorded on a Hitachi U-3010 spectrophotometer fitted with an integrating sphere with $BaSO_4$ as the reference. X-ray photoelectron spectroscopy (XPS) spectra were conducted at a Thermo Fisher ESCALAB 250Xi XPS microprobe with Al K_α radiation. Electron paramagnetic resonance (EPR) spectra were recorded on a Bruker EMXnano EPR spectrometer.

Photocatalytic H_2O_2 production

The photocatalytic reactions were performed in a double-layered 700 mL reactor equipped with a quartz window under 300 W Xe lamp. Typically, 50 mg catalyst powder was added to 100 mL aqueous solution with or without 2% HCOOH, then the reactor was sealed and irradiated under magnetic stirring. The temperature was controlled at 25 °C by circulating water. Before photoirradiation, the reaction solution was bubbled by O_2 or Ar or air for 30 min in the dark to obtain gas-saturated mixture. The concentration of H_2O_2 was determined by the titanium sulfate spectrophotometric method. To determine the amount of H_2O_2 during the photocatalytic reaction, 1 mL of the suspension was filtrated from the reactor every 30 min. Then 100 μL titanium sulfate and 2 mL sulfate were added into the above filtrate. After 10 min, the absorbance of the solution was recorded on a Hitachi U-3010 UV-vis spectrophotometer to quantify the amount of H_2O_2. Atmospheric experiments were carried out by the same procedure except that the air in the reactor was exhausted by O_2 or Ar for 30 min before reaction.

Electrochemical and photoelectrochemical measurement

The photocurrent response curves and electrochemical impedance spectroscopy (EIS) was measured on a Chenhua CHI-660D electrochemical workstation using a three-electrode system: Ag/AgCl reference electrode, Pt plate counter electrode, and photocatalyst-supporting FTO working electrode and a 300 W Xe lamp served as light source. The FTO glass was coated with 100 μL suspension (10 mg of sample was ultrasonically dispersed into 1 mL of 10 vol% Nafion (diluted with ethanol)), next dried at 80 °C for 1h as working electrode. Sodium sulfate (0.1 M, pH=6.8) was used as the electrolyte.

Photocatalytic degradation of RhB

Typically, 50 mg catalyst powder was added to 100 mL aqueous RhB dye solution (10 mg/L, 20 mg/L, 30 mg/L), then the reactor was sealed and irradiated under magnetic stirring. The temperature was controlled at 25 °C by circulating water. Before photoirradiation, the reaction solution was bubbled by O_2 or air for 30 min in

the dark to obtain gas-saturated mixture. The mixture was irradiated under 300 W Xe lamp and 2 mL of the suspension was filtrated from the reactor every 2 min. The concentration of RhB was recorded on Hitachi U-3010 UV-vis spectrophotometer at 555 nm by measuring absorbance.

Reactive oxygen species detection

Utilizing the 5,5-dimethyl-1-pyrroline-N-oxide (DMPO) as the trapping agent, •OH and $\bullet O_2^-$ were detected by EPR experiments. Utilizing the TEMP as the trapping agent, $^1O_2$ was detected by EPR. In detail, the detection of •OH and $\bullet O_2^-$ were carried out in deionized water and chromatographically pure methanol containing DMPO and the catalysts. The detection of of $^1O_2$ were carried out in deionized water with TEMP and the catalysts. The radicals were detected without and with light irradiation for 3 min.

The apparent quantum efficiency (AQE) test

The AQY test used a LED lamp of 390 nm. The concentration of photocatalyst in the solution (2 % HCOOH) was 50 mg/100 mL. The AQE was calculated by the following formula:

$$AQE = \frac{2 * H2O2\ formed\ (mol)}{the\ number\ of\ incident\ photos\ (mol)}$$

The solar- to-chemical conversion efficiency (SCC) test

The SCC efficiency test was carried with the photocatalyst in 2% HCOOH (0.5 g/L, 100 mL) and LED lamp (390 nm). The SCC efficiency was calculated by the following formula:

$$SCC = \frac{(\Delta GH2O2) * (nH2O2)}{I * S * T} * 100\%$$

Where ΔG_{H2O2}, n_{H2O2}, I, S, and T resent the free energy for H_2O_2 generation (117 KJ/mol), the molar amount of H_2O_2 generated, the energy intensity of the LED solar irradiation (1370 W/m^2), the irradiated sample area and the irradiation time (s), respectively.

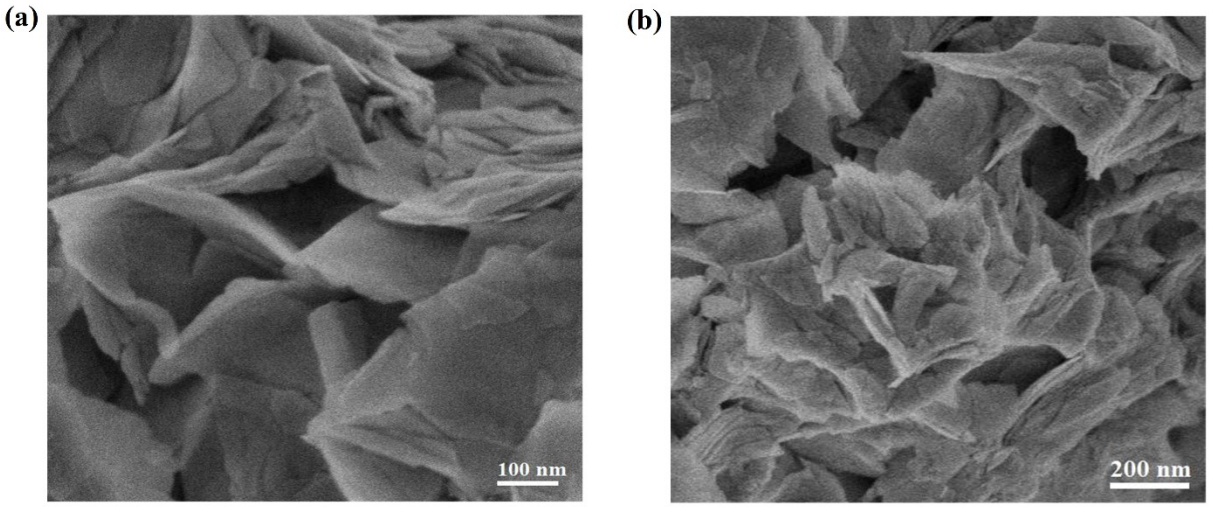

90

91 **Fig. S1.** SEM images of BiOBr.

92

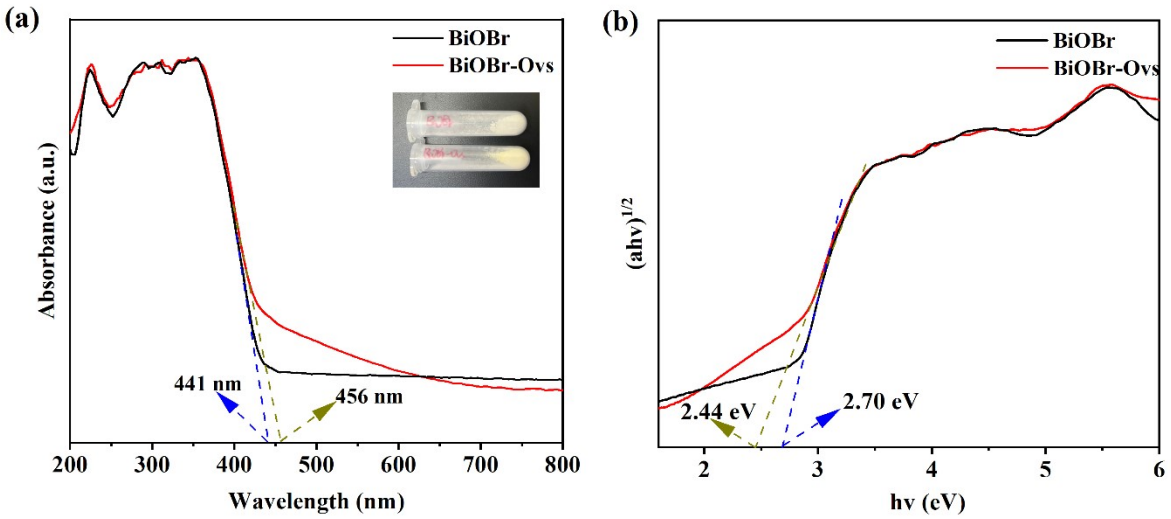

93

94 **Fig. S2.** Characterization for band diagram construction. (a) DRS spectra; (b) Tauc

95 plots.

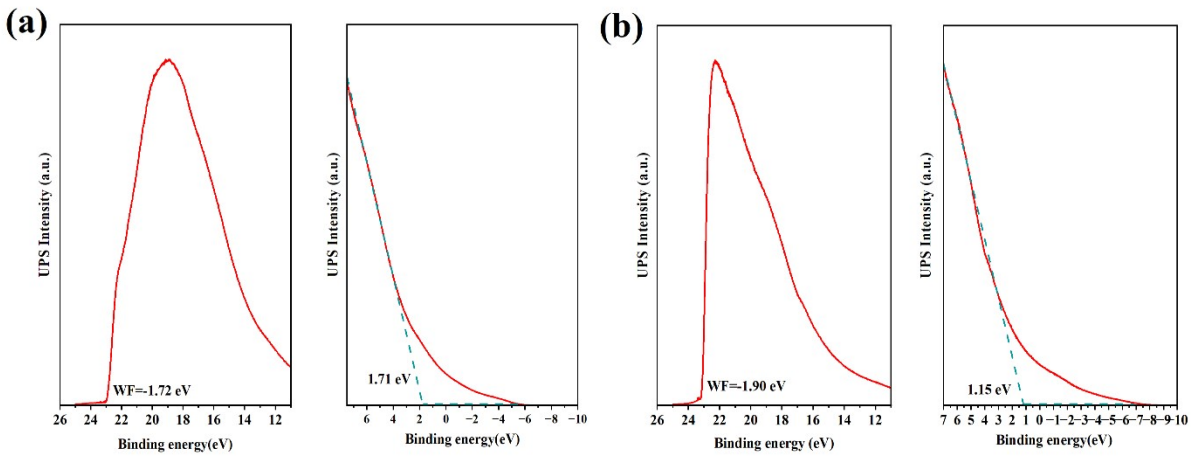

Fig. S3. UPS spectra of photocatalysts. (a) BiOBr; (b) BiOBr-Ovs. The intersections of the tangents with the baseline give the edges of the UPS spectra from which the UPS width is determined.

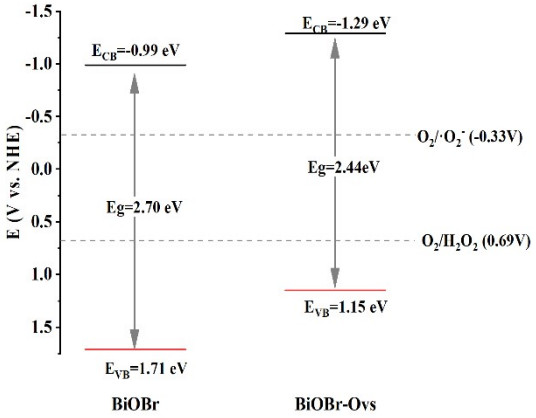

Fig. S4. Band structure alignments of BiOBr and BiOBr-Ovs.

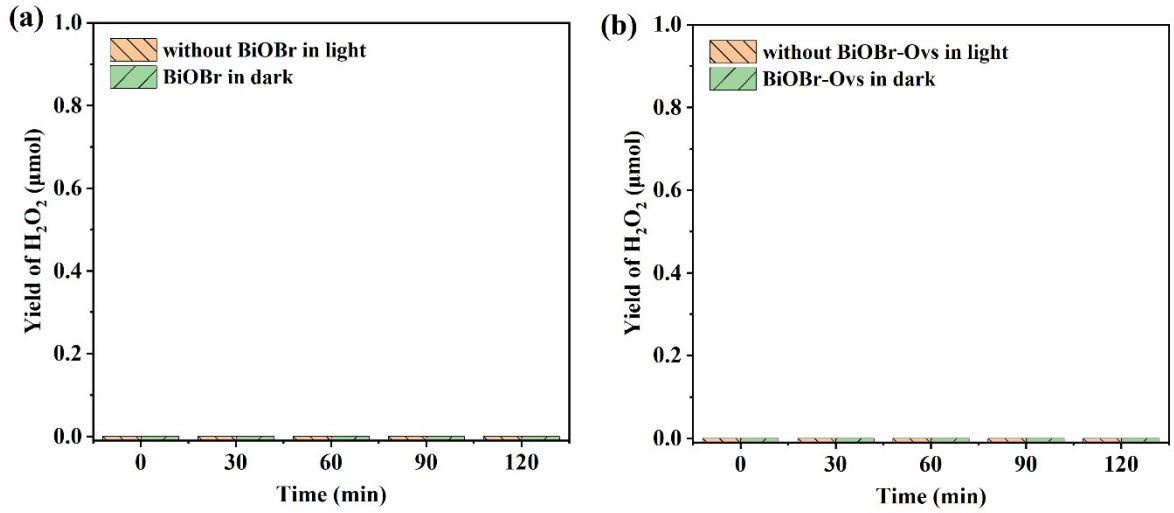

104

105 **Fig. S5.** Control experiments results. (a) H_2O_2 yields over BiOBr without light
106 irradiation and without photocatalysts. (b) H_2O_2 yields over BiOBr-Ovs without light
107 irradiation and without photocatalysts. Reaction conditions: O_2 atmosphere, 50 mg
108 photocatalysts, 100 mL H_2O, and 300 W Xe lamp.

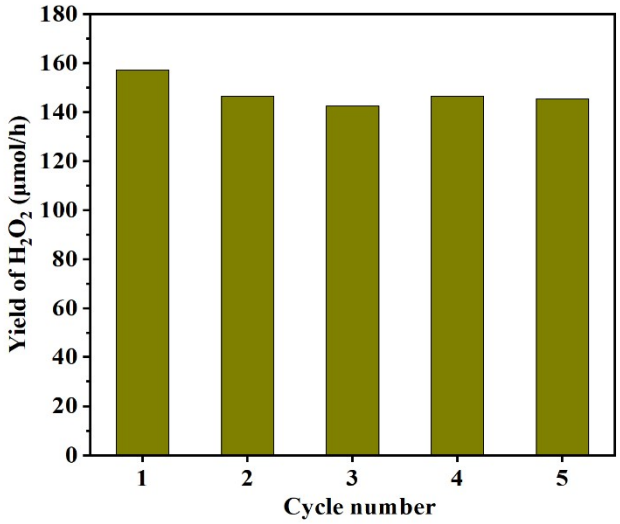

109

110 **Fig. S6.** Photocatalytic stability of BiOBr-Ovs under visible-light irradiation in 2%
111 HCOOH. Reaction conditions: O_2 atmosphere, 50 mg photocatalysts, 100 mL 2%
112 HCOOH solution, and 300 W Xe lamp.

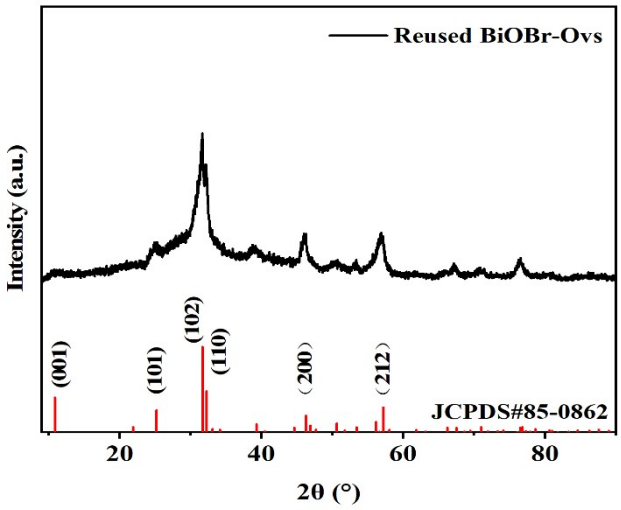

113

114 **Fig. S7.** XRD pattern of BiOBr-Ovs after circulation.

115

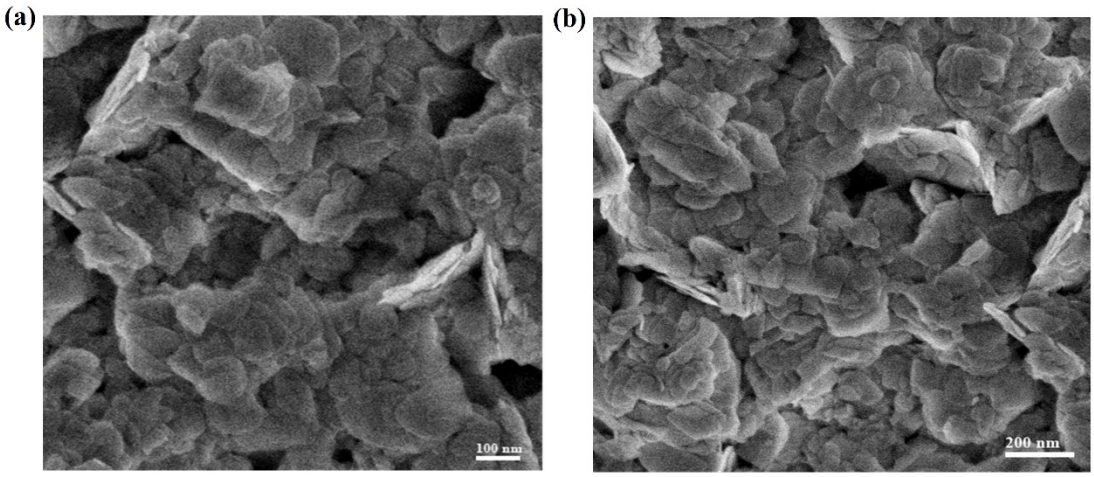

116

117 **Fig. S8.** SEM images of BiOBr-Ovs after circulation.

118

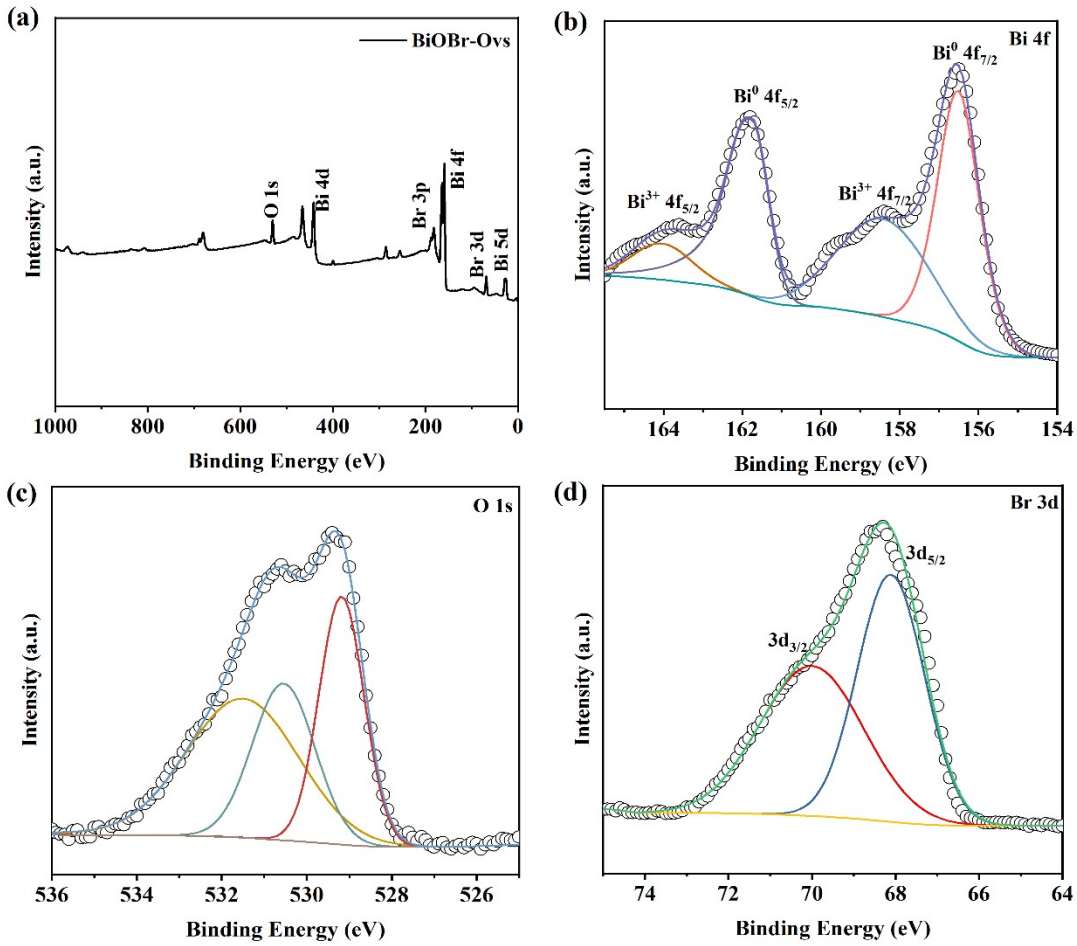

Fig. S9. XPS characterizations of BiOBr-Ovs after circulation. (a) survey XPS spectrum; (b) Bi 4*f* spectrum; (c) O 1*s* spectrum; (d) Br 3*d* spectrum.

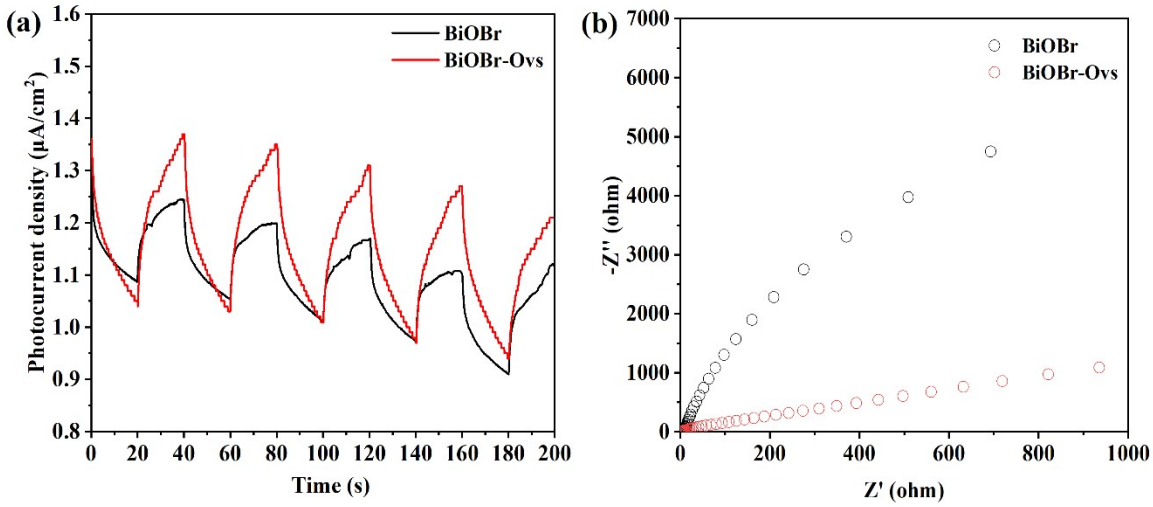

Fig. S10. (a) Transient photocurrent responses of the photocatalysts; (b) EIS spectra

of BiOBr and BiOBr-Ovs.

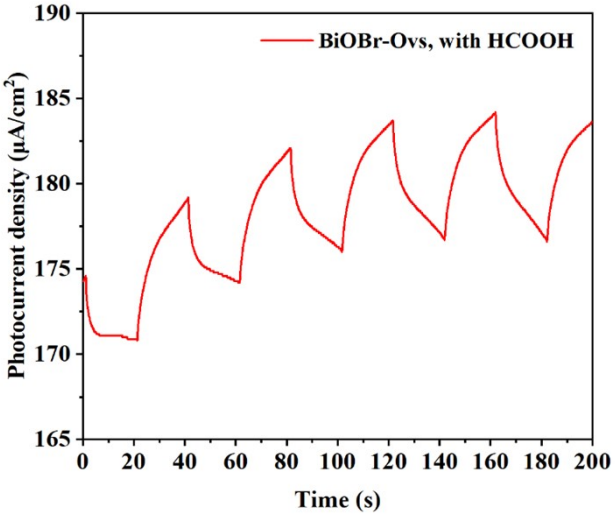

Fig. S11. Transient photocurrent response of the BiOBr-Ovs with HCOOH.

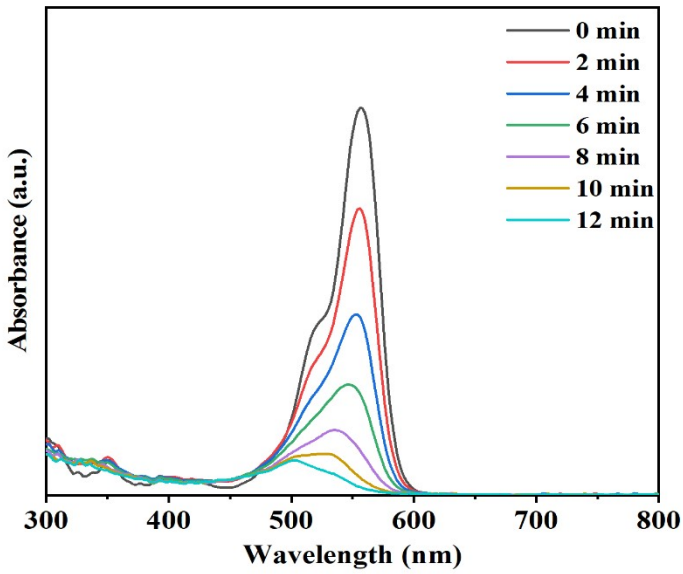

Fig. S12. UV-vis absorption spectra of the RhB at different irradiation time.

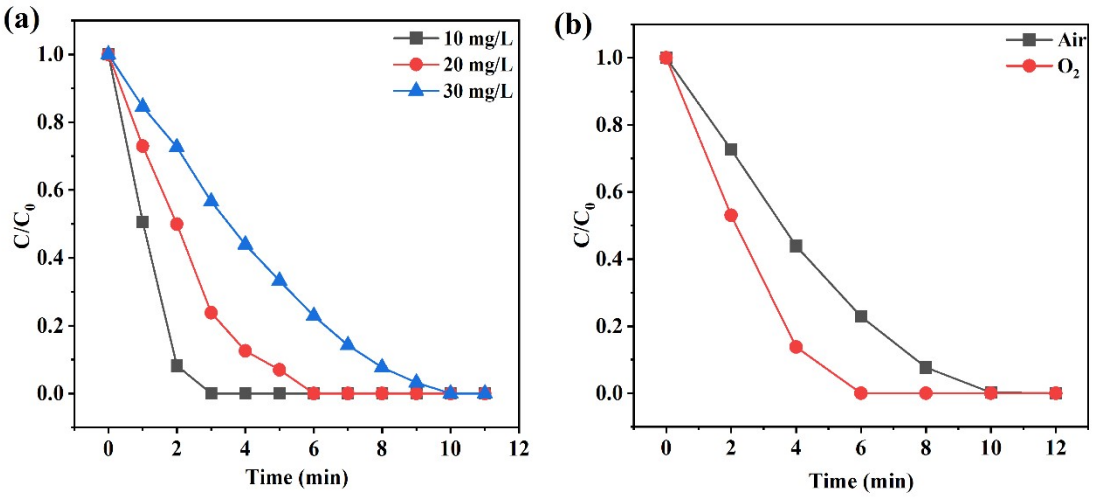

Fig. S13. (a) Comparison of RhB degradation with different concentration; (b) Comparison of RhB degradation in different atmosphere.

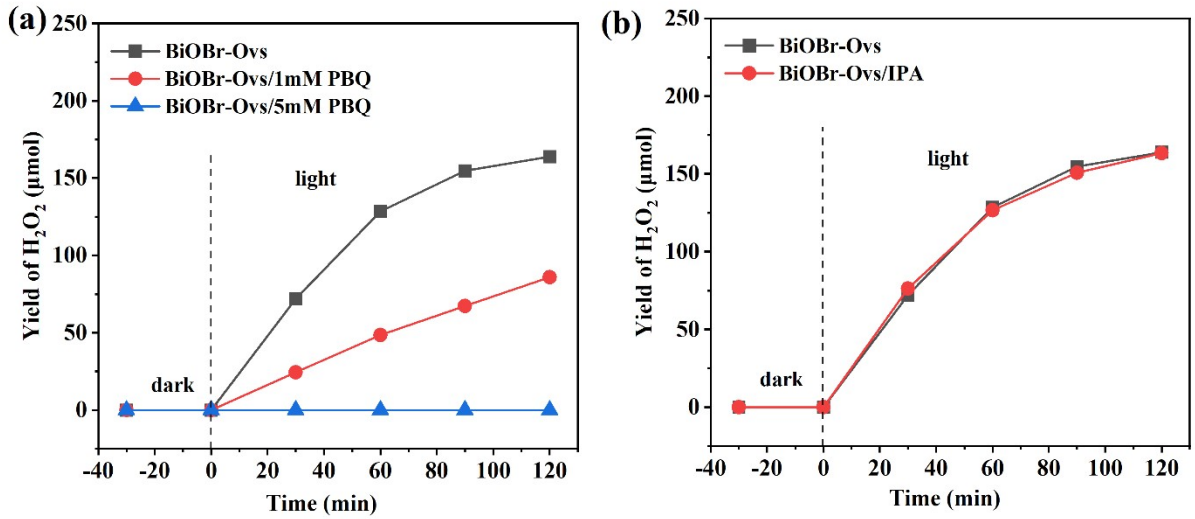

Fig. S14. The influence of $\bullet O_2^-$ and •OH scavengers on the photocatalytic H_2O_2 production over BiOBr-Ovs. (a) PBQ; (b) IPA.

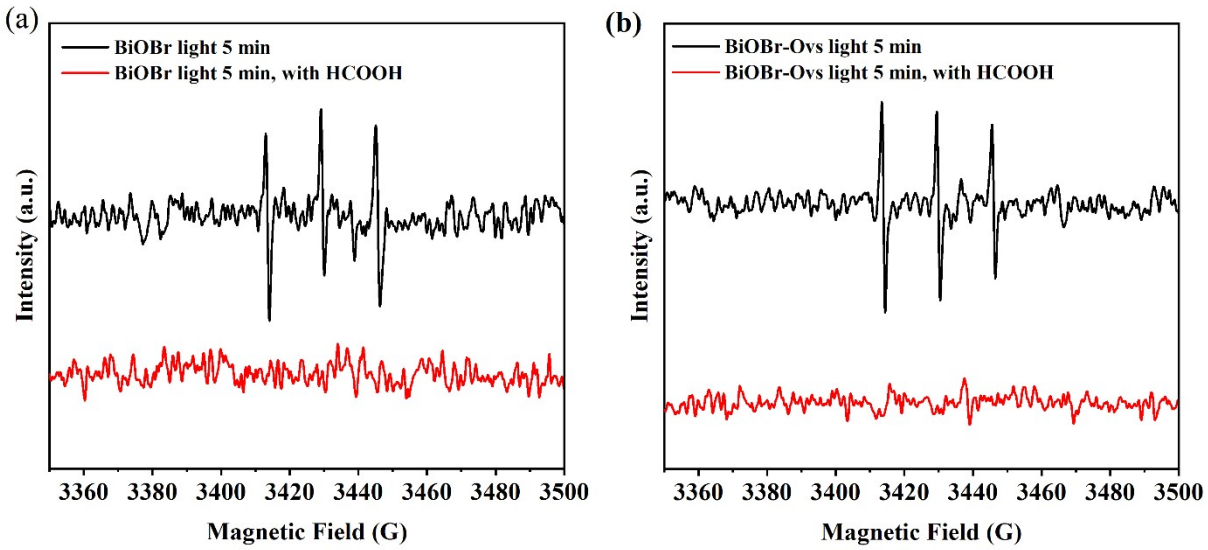

139

140 **Fig. S15.** EPR spectra of radical species. (a) TEMP-$^1O_2$ for BiOBr under light
141 illumination with and without HCOOH; (b) TEMP-$^1O_2$ for BiOBr-Ovs under light
142 illumination with and without HCOOH.

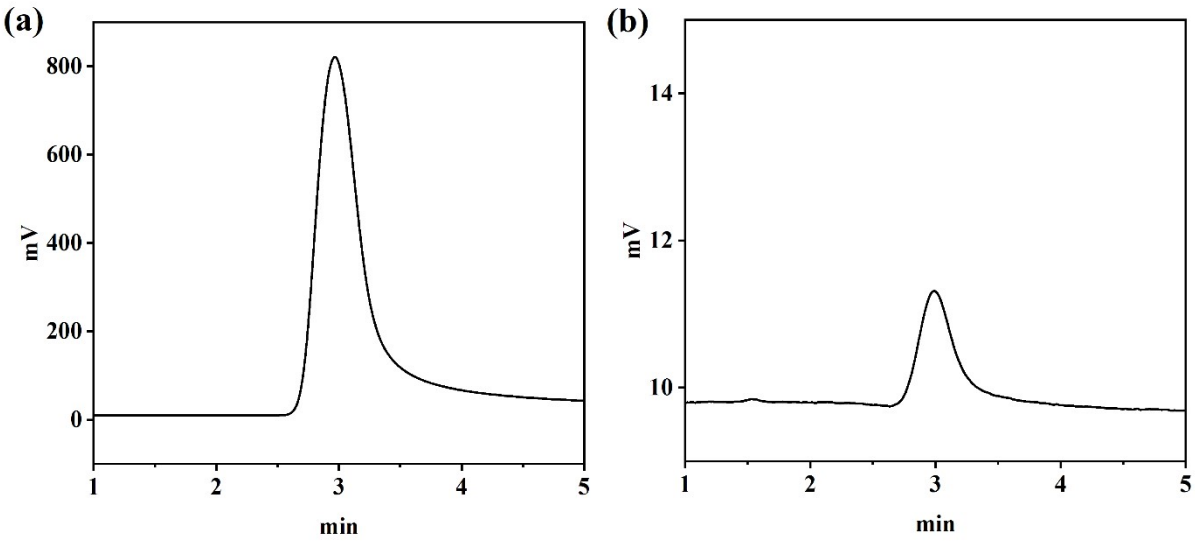

143

144 **Fig. S16.** Gas chromatogram of CO_2. (a) Pure CO_2; (b) Gas in the reactor after the
145 reaction.

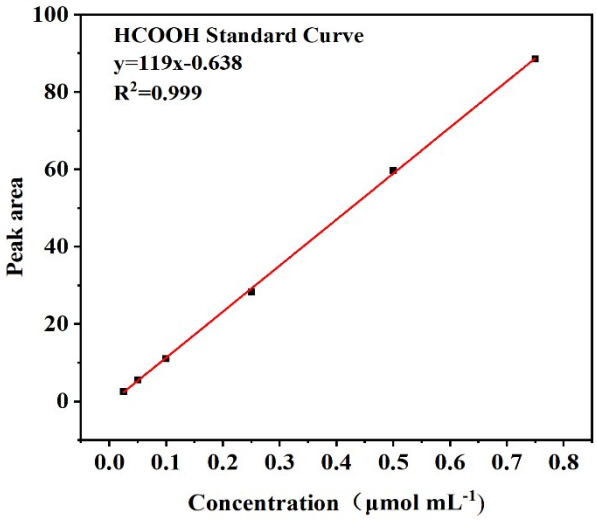

146

147 **Fig. S17.** The calibration curve used for estimation of HCOOH concentration.

148

149 **Table S1** List of some state-of-the-art photocatalytic H_2O_2 production systems

150 without sacrificial agents.

Photocatalysts	Solution	Atmosphere	Light Source	H_2O_2 Production ($\mu mol \cdot h^{-1}$)	Ref.
BiOBr-Ovs	**H_2O**	**O_2**	**300 W Xe**	**3.0**	**This**
		Air	**lamp**	**1.5**	**Work**
PCN/PDI	H_2O	O_2	2000 W Xe lamp	1.05	1
Au/$BiVO_4$	H_2O	O_2	2000 W Xe lamp	0.12	2
PCN/BDI	H_2O	O_2	2000 W Xe lamp	0.85	3
PCN	H_2O	Air	300 W Xe lamp	0.65	4
PCN	H_2O	Air	300 W Xe lamp	1.3	5

CTF-BPDCN	H_2O	O_2	300 W Xe lamp	0.88	6

Table S2 List of some state-of-the-art photocatalytic H_2O_2 production systems with sacrificial agents.

Photocatalysts	Solution	Atmosphere	Light Source	H_2O_2 Production ($\mu mol \cdot h^{-1}$)	Ref.
BiOBr-Ovs	**2% formic acid**	**O_2**	**300 W Xe lamp**	**150**	**This Work**
10%BP/CN	10% isopropyl alcohol	O_2	300 W Xe lamp	27	7
g-C_3N_4-CNTs	5% formic acid	O_2	300 W Xe lamp	32.6	8
$CNK_{0.2}$	5% methanol	O_2	300 W Xe lamp	101	9
PCN-$K_{1.0}$	10% ethanol	O_2	300 W Xe lamp	40	10
Ti_2C_3/g-C_3N_4/BiOCl	5% isopropyl alcohol	O_2	300 W Xe lamp	63.75	11

Reference

1 Y. Shiraishi, S. Kanazawa, Y. Kofuji, H. Sakamoto, S. Ichikawa, S. Tanaka and T. Hirai, *Angew. Chem. Int. Ed.*, 2014, **53**, 13454-13459.

2 H. Hirakawa, S. Shiota, Y. Shiraishi, H. Sakamoto, S. Ichikawa and T. Hirai, *ACS Catal*., 2016, **6**, 4976-4982.

3 Y. Kofuji, S. Ohkita, Y. Shiraishi, H. Sakamoto, S. Tanaka, S. Ichikawa and T. Hirai, *ACS Catal.*, 2016, **6**, 7021-7029.

4 S. Li, G. Dong, R. Hailili, L. Yang, Y. Li, F. Wang, Y. Zeng and C. Wang, *Appl. Catal. B,* 2016, **190**, 26-35.

5 S. Zhao, X. Zhao, H. Zhang, J. Li and Y. Zhu, *Nano Energy*, 2017, **35**, 405-414.

6 L. Chen, L. Wang, Y. Wan, Y. Zhang, Z. Qi, X. Wu and H. Xu, *Adv Mater*, 2020, **32**, e1904433.

7 Y. Zheng, Z. Yu, H. Ou, A. M. Asiri, Y. Chen and X. Wang, *Adv. Funct. Mater.,* 2018, **28**, 1705407.

8 S. Zhao, T. Guo, X. Li, T. Xu, B. Yang and X. Zhao, *Appl. Catal. B,*, 2018, **224**, 725-732.

9 Y. Wang, D. Meng and X. Zhao, *Appl. Catal. B,* 2020, **273**, 119064.

10 J. Tian, D. Wang, S. Li, Y. Pei, M. Qiao, Z.-H. Li, J. Zhang and B. Zong, *ACS Sustain. Chem. Eng.,* 2019, **8**, 594-603.

11 Q. Yang, R. Li, S. Wei and R. Yang, *Appl. Surf. Sci.*, 2022, **572**, 151525.